Journal of Biomolecular NMR, **26:** 39–48, 2003.
KLUWER/ESCOM

Off-resonance $R_{1\rho}$ relaxation outside of the fast exchange limit: An experimental study of a cavity mutant of T4 lysozyme

Dmitry M. Korzhnev[a], Vladislav Yu. Orekhov[b], Frederick W. Dahlquist[c] & Lewis E. Kay[a]
[a]*Protein Engineering Network Centers of Excellence and Departments of Medical Genetics, Biochemistry and Chemistry, University of Toronto, Toronto, Ontario M5S 1A8, Canada*
[b]*Swedish NMR Centre at Göteborg University, Box 465, 405 30 Göteborg, Sweden*
[c]*Institute of Molecular Biology and Department of Chemistry, University of Oregon, Eugene, Oregon 97403, U.S.A.*

Received 6 December 2002; Accepted 31 January 2003

Key words: conformational exchange, ^{15}N relaxation dispersion spectroscopy, offset-dependence of $R_{1\rho}$, T4 lysozyme

Abstract

An ^{15}N off-resonance $R_{1\rho}$ spin relaxation study of an L99A point mutant of T4 lysozyme is presented. Previous CPMG-based relaxation dispersion studies of exchange in this protein have established that the molecule interconverts between a populated ground state and an excited state (3.4%) with an exchange rate constant of 1450 s^{-1} at 25 °C. It is shown that for the majority of residues in this protein the offset dependence of the $R_{1\rho}$ relaxation rates cannot be well fit using models which are only valid in the fast exchange regime. In contrast, a recently derived expression by Trott and Palmer (*J. Magn. Reson.*, **154**, 157–160, 2002) which is valid over a wider window of exchange than other relations, is shown to fit the data well. Values of (signed) chemical shift differences between exchanging sites have been extracted and are in reasonable agreement with shift differences measured using CPMG methods. A set of simulations is presented which help establish the exchange regimes that are best suited to analysis by off-resonance $R_{1\rho}$ techniques.

Introduction

The ability of proteins to access different conformations is essential to their function. Many conformational transitions in proteins occur on a micro- to millisecond time scale (Akke, 2002), leading to line broadening in NMR spectra and enhancement of measured transverse relaxation rates. In practice quantification of such processes involves measuring rotating frame relaxation rates, $R_{1\rho}$, as a function of the strength and/or carrier frequency of the applied RF field (Peng et al., 1991; Szyperski et al., 1993; Akke and Palmer, 1996; Zinn-Justin et al., 1997; Mulder et al., 1998) or transverse relaxation rates, R_2, as a function of pulse repetition rates in CPMG sequences (Orekhov et al., 1994; Loria et al., 1999a, b; Tollinger et al., 2001; Mulder et al., 2001b; Skrynnikov et al., 2001).

CPMG based methods for studying conformational exchange in proteins are now well established (Palmer et al., 2001). Experiments have been developed for measuring dispersions of relaxation rates of ^{15}N spins in NH (Loria et al., 1999a, b; Tollinger et al., 2001) and NH_2 (Mulder et al., 2001b) moieties as well as of ^{13}C spins in CH_3 groups (Skrynnikov et al., 2001; Mulder et al., 2002), allowing a detailed description of conformational exchange at a large number of sites in a given protein. In the case of two site exchange, for example, and in favorable situations, it is possible to measure the populations of the two exchanging states along with exchange rates and the absolute value of the shift differences, $\Delta\omega$, between the states. Very recently it has been shown that the sign of $\Delta\omega$ can be obtained from exchange-induced line shifts in HMQC and HSQC spectra (Skrynnikov et al., 2002). The rate constants and populations extracted from CPMG data provide valuable thermodynamic

information about exchanging conformations, while $\Delta\omega$ values are critical for understanding the structural changes that accompany the exchange process. In a series of recent publications CPMG dispersion measurements were applied to characterize transitions to low-populated excited state conformations of a cavity mutant of T4 lysozyme (Mulder et al., 2001a) and of azurin (Korzhnev et al., 2003).

CPMG dispersion measurements fail in applications where the exchange rates are beyond the accessible range of CPMG frequencies, $\omega_{CPMG} = 2\pi\nu_{CPMG} = \pi/\tau_{CPMG}$, with τ_{CPMG} the time between π pulses of the CPMG sequence. For typical ω_{CPMG} values between approximately 300–6,000 radians/sec (ν_{CPMG} of 50 Hz–1 kHz), quantification is most reliable for processes with time constants on the order of hundreds of microseconds to several milliseconds. Rotating-frame relaxation ($R_{1\rho}$) measurements are an excellent alternative to CPMG based methods when conformational exchange processes occur on faster time scales. These experiments are best suited for studying conformational exchange with rates on the order of the effective RF field strength, ω_e (radians/sec) given by $(\omega_1^2 + \delta^2)^{1/2}$, where ω_1 is the spin-lock field strength and δ is the resonance offset from the spin-lock carrier. Typically, in $^{15}N/^{13}C$ off-resonance $R_{1\rho}$ experiments one employs ω_1 fields of approximately 6,000–13,000 radians/sec ($\nu_1 = \omega_1/(2\pi)$ of 1.0–2.0 kHz) and samples ranges of $\delta/(2\pi)$ of approximately $\pm$5 kHz. Thus, ω_e values range from ~6,000 to ~35,000 and fast conformational exchange processes on the microsecond timescale, which are inaccessible to CPMG dispersion experiments, can be studied.

In the past few years considerable advances have been made in both the theory and the experiments for studying conformational exchange in proteins using $R_{1\rho}$ relaxation. Improved experimental schemes employing adiabatic rotations have been implemented for magnetization alignment along the effective field in the rotating frame (Mulder et al., 1998), and new methods have been introduced for suppression of dipole–CSA cross-correlation during the spin-lock period which correct problems associated with previous schemes (Korzhnev et al., 2002). Almost all $R_{1\rho}$ studies of proteins to date make the assumption of fast exchange (Davis et al., 1994) and extracted parameters are likely biased in cases where this is violated. Recently Trott and Palmer (2002) have derived a new general expression for $R_{1\rho}$ in systems undergoing two-site exchange which is valid outside the limit of fast exchange, and in a subsequent paper have modified this expression to provide accurate $R_{1\rho}$ rates when exchange is not fast and populations of exchanging states are close to equal (Trott et al., 2003). In principle, this expression allows extraction of populations, rates and $\Delta\omega$ from $R_{1\rho}$ data measured at a single magnetic field strength, thus providing a complete kinetic and thermodynamic description of the exchange process.

To the best of our knowledge experimental verification of the Trott/Palmer theory has not appeared in the literature. Here we show that the Trott/Palmer equation is able to properly fit ^{15}N $R_{1\rho}$ data recorded on an L99A mutant of T4 lysozyme, L99A (Eriksson et al., 1992), while equations which assume fast chemical exchange fail completely. It is shown experimentally that fits to the Trott/Palmer equation allow extraction of the sign of $\Delta\omega$, as predicted previously (Trott and Palmer, 2002). Finally, numerical simulations are presented which probe the sensitivity of the exchange parameters extracted from $R_{1\rho}$ data in different exchange regimes to experimental errors.

Theory

Consider an exchange process between states A and B with populations p_A and p_B and with forward and reverse rate constants k_A and k_B, respectively ($k_A = k_{ex}p_B$, $k_B = k_{ex}p_A$, $k_{ex} = k_A + k_B$). For a spin with Larmor frequency Ω_A in state A and Ω_B in state B the evolution of magnetization is given by the Bloch–McConnel equation (McConnell, 1958):

$$\frac{d}{dt}\mathbf{M}(t) = \mathbf{R}\mathbf{M}(t) + R_1\mathbf{M}_0, \tag{1}$$

where $\mathbf{M} = (M_{Ax}, M_{Bx}, M_{Ay}, M_{By}, M_{Az}, M_{Bz})^T$ and $\mathbf{M}_0 = (0, 0, 0, 0, M_{A0}, M_{B0})^T$ are vectors consisting of magnetization components for spins in states A and B at time t and at equilibrium, respectively, and M_{A0} and M_{B0} are proportional to p_A and p_B. The matrix $\mathbf{R}$ describing evolution of the system under an RF spin-lock field of strength ω_1 applied along the X-axis is given by:

$$\mathbf{R} = -\begin{pmatrix} R_2 + k_A & -k_B & \delta_A & 0 & 0 & 0 \\ -k_A & R_2 + k_B & 0 & \delta_B & 0 & 0 \\ -\delta_A & 0 & R_2 + k_A & -k_B & \omega_1 & 0 \\ 0 & -\delta_B & -k_A & R_2 + k_B & 0 & \omega_1 \\ 0 & 0 & -\omega_1 & 0 & R_1 + k_A & -k_B \\ 0 & 0 & 0 & -\omega_1 & -k_A & R_1 + k_B \end{pmatrix} \tag{2}$$

where $\delta_A = \Omega_A - \Omega_{SL}$ and $\delta_B = \Omega_B - \Omega_{SL}$ are the resonance offsets from the spin-lock carrier Ω_{SL} for the exchanging spin in states A and B, respectively. Note that Equations 1 and 2 are written assuming that the intrinsic relaxation rates (R_1 and R_2) in both states are identical. The solution to Equation 1 requires calculation of the eigenvalues and eigenvectors for the 6×6 matrix **R** (Equation 2) which, in turn, involves finding the roots of a 6th power polynomial. This significantly complicates derivation of the exact analytic expression for the evolution of **M**(t).

It can be shown that for typical experimental conditions four of the six eigenvalues of the evolution matrix **R** (Equation 2) are complex numbers with a relatively large imaginary part, while the two remaining values are real and negative (Trott and Palmer, 2002). Creation of the oscillatory components of **M**(t) which evolve with frequencies given by the imaginary parts of complex eigenvalues can be prevented by using adiabatic pulses which rotate the magnetization from the Z-axis to the effective field before the spin lock period and subsequently back to the Z-axis after this interval (see Methods). Moreover, if created such components would deteriorate rapidly due to ω_1 field inhomogeneity. In many cases of interest the two real eigenvalues of **R** are significantly different in magnitude (Trott and Palmer, 2002). In these cases the evolution of magnetization is essentially mono-exponential, **M**(t)$\sim$exp(λt), with λ given by the least negative real eigenvalue.

Although calculation of the eigenvalues of **R** is easily done numerically it would be convenient to have a compact approximate expression for $R_{1\rho} = -\lambda$. Such an expression, valid in the case of exchange occurring much faster than relaxation ($k_{ex} \gg R_1, R_2$), has been derived recently by Trott and Palmer (Trott and Palmer, 2002):

$$R_{1\rho} = R_1 \cos^2\theta + (R_2 + R_{ex}) \sin^2\theta, \tag{3}$$

where

$$R_{ex} = \frac{p_A p_B \Delta\omega^2 k_{ex}}{\omega_{Ae}^2 \omega_{Be}^2 / \omega_e^2 + k_{ex}^2} \tag{4}$$

$\theta = \text{arccot}(\delta/\omega_1)$, $\omega_{Ae} = (\omega_1^2 + \delta_A^2)^{1/2}$, $\omega_{Be} = (\omega_1^2 + \delta_B^2)^{1/2}$, $\omega_e = (\omega_1^2 + \delta^2)^{1/2}$, $\delta_A = \Omega_A - \Omega_{SL}$, $\delta_B = \Omega_B - \Omega_{SL}$, $\delta = \Omega - \Omega_{SL}$, $\Omega = p_A\Omega_A + p_B\Omega_B$, $\Delta\omega = \delta_B - \delta_A = \Omega_B - \Omega_A$. It can be shown that (i) in the fast exchange limit, $k_{ex} \gg |\Delta\omega|$ or (ii) in the limit of a large spin-locking field with $\omega_1 \gg |\Delta\omega|$, Equation 4 reduces to the expression derived earlier by Davis et al. (1994):

$$R_{ex} = \frac{p_A p_B \Delta\omega^2 k_{ex}}{\omega_e^2 + k_{ex}^2}. \tag{5}$$

In the asymmetric population limit, $p_A \gg p_B$, Equation 4 can be written as:

$$R_{ex} = \frac{p_B \Delta\omega^2 k_{ex}}{\omega_{Be}^2 + k_{ex}^2}. \tag{6}$$

The $R_{1\rho}$ rates given by Equations 3 and 4 depend on the exchange parameters, k_{ex}, p_A ($p_B = 1 - p_A$) and $\Delta\omega$ as well as other parameters including the intrinsic relaxation rates, R_1, R_2, the spin-lock field strength, ω_1, and the resonance frequencies for sites A and B, Ω_A and Ω_B. Usually k_{ex}, p_A, $\Delta\omega$ and R_2 are adjusted during the course of $R_{1\rho}$ data fitting while R_1, ω_1 and information about chemical shifts (for example Ω, see below) are obtained from independent experiments. ^{15}N R_1 values can be measured using very sensitive experiments (Farrow et al., 1994), while the strength of the spin lock field, ω_1, is obtained from the 90° pulse length or, more precisely, from the distribution of B_1 fields measured as described previously (Guenneugues et al., 1999). In the fast exchange limit, $k_{ex} \gg |\Delta\omega|$, a single coalescence peak is observed at $\Omega = p_A\Omega_A + p_B\Omega_B$ so that this value (and hence δ) can be estimated directly. In the intermediate to slow exchange regimes there are separate peaks for each spin in sites A and B and their positions depend on the exchange parameters and hence can be used to extract these parameters in the first place. The shifts in peak positions (in the free precession limit) can be calculated using the expression for evolution of transverse magnetization in a system undergoing two-site exchange:

$$\frac{d}{dt}\begin{pmatrix} M_{A+}(t) \\ M_{B+}(t) \end{pmatrix} = \begin{pmatrix} -i\Omega_A - k_A - R_2 & k_B \\ k_A & -i\Omega_B - k_B - R_2 \end{pmatrix}\begin{pmatrix} M_{A+}(t) \\ M_{B+}(t) \end{pmatrix}, \tag{7}$$

where $M_{A+} = M_{Ax} + iM_{Ay}$, $M_{B+} = M_{Bx} + iM_{By}$, with the peak positions given by the imaginary parts of the eigenvalues of the 2×2 evolution matrix of Equation 7. In the asymmetric population limit, $p_A \gg p_B$, a resonance from spins in state A is observed at

$$\Omega'_A = \Omega_A + \frac{p_B k_{ex}^2 \Delta\omega}{\Delta\omega^2 + k_{ex}^2}, \tag{8}$$

while the resonance corresponding to spins in the minor state B is often not detected. The values of Ω'_A can be measured directly from the experiment and Ω_A calculated during the course of the fitting from Equation 8 (or 7).

In the fast exchange limit (Equation 5) the parameters that can be extracted from fits of the ω_e dependence of $R_{1\rho}$ data are k_{ex} and the product $p_A p_B \Delta\omega^2$ and these values are essentially what have been reported in the literature to date. In principle, however, the Trott/Palmer formula (Equation 4) allows a determination of all exchange parameters, k_{ex}, p_A (p_B) and $\Delta\omega$, using $R_{1\rho}$ data measured at a single magnetic field strength in favorable cases (i.e., if it is *not* the case that $k_{ex} \gg |\Delta\omega|$ or $\omega_1 \gg |\Delta\omega|$, for example). Another potentially interesting situation is the one with asymmetric populations $p_A \gg p_B$ (see Equation 6) and where $k_{ex}^2 \ll \omega_1^2$; this is the case in the present study of L99A. In this case Equation 6 does not depend on p_B and k_{ex} separately but only on their product $p_B k_{ex}$ since the denominator is essentially independent of k_{ex}. This reduces the set of exchange parameters that can be extracted from $R_{1\rho}$ data to $p_B k_{ex}$ and Ω_A, Ω_B. (Although at first glance it might appear that p_B and k_{ex} can be separated using Equations 6 and 8 in combination, in practice this is very difficult to achieve since $\Omega'_A \approx \Omega_A$).

As described above, for an exchanging system outside the fast exchange limit it is possible to obtain not only the magnitude of the chemical shift difference $|\Delta\omega|$ but also the sign of the difference from fits of $R_{1\rho}$ relaxation data to the expression of Trott and Palmer (2002). This information is of particular interest in the asymmetric population case, $p_A \gg p_B$, where resonances of the low-populated state are not detectable. In principle, based on the resonance positions for the ground state and $\Delta\omega$ values obtained from $R_{1\rho}$ data it is possible to reconstruct the spectrum of the 'invisible' conformer. In the limit that $p_A \gg p_B$ the maximum of R_{ex} (Equation 6) occurs when the spin-lock carrier frequency Ω_{SL} is at the Larmor frequency of the minor state Ω_B (i.e., at $\delta_B = \Omega_B - \Omega_{SL} = 0$). Thus, the $R_{1\rho}$ maximum (see Equations 1 and 2) is shifted with respect to $\Omega = p_A\Omega_A + p_B\Omega_B$ towards Ω_B. On the other hand, the spins in the ground state (state A) resonate at Ω'_A, between Ω_A and Ω (see Equation 8). Therefore, the shift of the $R_{1\rho}$ maximum with respect to the ground state peak position (Ω'_A) clearly establishes the sign of $\Delta\omega = \Omega_B - \Omega_A$.

Methods

R_1 and off-resonance $R_{1\rho}$ relaxation rates were measured for backbone ^{15}N spins of a 1.5 mM sample of T4 lysozyme (with the mutations C54T/C97A/L99A), 50 mM sodium phosphate, 25 mM sodium chloride, pH 5.5. All spectra were collected at 25 °C on a Varian *Inova* spectrometer operating at 800 MHz (^{1}H frequency). The ^{15}N R_1 and $R_{1\rho}$ experiments were carried out as described previously (Farrow et al., 1994; Mulder et al., 1998; Korzhnev et al., 2002). $R_{1\rho}$ data sets were recorded with 110 and 832 complex data points in t_1,t_2 corresponding to acquisition times of 36.7 and 65.4 ms in the ^{15}N and ^{1}HN dimensions, respectively. A relaxation delay of 1.8 s was employed, along with 8 scans/FID to give an acquisition time of 57 min/spectrum and a net measuring time (56 data sets) of approximately 53 h for each spin-lock field strength that was employed (i.e., for each value of ω_1, see below).

In the $R_{1\rho}$ experiment the magnetization of each ^{15}N spin was rotated adiabatically from the Z-axis to the appropriate effective field using a frequency and amplitude modulated pulse, $\omega(t) = \omega_0[\tan(\arctan(50)[1 - t/\tau])]/50$ and $\omega_1(t) = \omega_1 \tanh(10t/\tau)$, with $\tau = 6$ ms, $\omega_0/2\pi = 30$ kHz and ω_1 is the spin-lock field strength (Mulder et al., 1998). A similar adiabatic pulse with time reversed modulation was used to rotate magnetization back to the Z-axis at the end of the spin-lock period.

$R_{1\rho}$ data were measured using two spin-lock field strengths, $\omega_1/(2\pi) = 805$ and 1136 Hz. The offset dependence of $R_{1\rho}$ was obtained on the basis of 51 points recorded with offsets $\Omega_0/2\pi$ ranging from -2.5 to 2.5 kHz, with $\Omega_0 = \Omega_{SL} - \Omega_{ref}$, where Ω_{ref} corresponds to the center of the ^{15}N spectrum (119 ppm). For $\Omega_0 \geqslant 0$ (26 data points spaced evenly between 0 and 2.5 kHz, including 0) the sweep direction of the adiabatic pulse was from downfield to upfield, starting 30 kHz downfield of Ω_{SL} and finishing at Ω_{SL}. An additional 25 spectra were acquired with $\Omega_0 < 0$ (Ω_0 spaced evenly between 0 and -2.5 kHz) and the sense of the sweep was reversed. In this way the frequency sweep of the adiabatic pulse never progresses past the center of the spectrum (Ω_{ref}) in any of the measurements. Simulations have established that all of the resonances in the spectrum are effectively spin-locked using this approach.

In principle, for each value of Ω_0 at least two spectra must be recorded with different spin-lock times. Subsequently $R_{1\rho}$ values can be calculated on

a per-residue basis from intensities I_1 and I_0 measured in the two spectra according to the relation

$$R_{1\rho} = -\frac{1}{T} \ln \frac{I_1}{I_0}, \quad (9)$$

where T is the difference in spin-lock durations. In practice, we have chosen an alternative approach, which maximizes the number of Ω_0 values that can be obtained per unit measuring time. For each value of Ω_0 a spectrum was recorded with a 60 ms spin-lock period, for which $I_1(\Omega_0)$ values are obtained for each residue. Subsequently 5 additional spectra were obtained with the spin-lock duration set to 0 ms and with $\Omega_0/2\pi$ values of 0, ± 1.25 and ± 2.5 kHz. The complete $I_0(\Omega_0)$ profile (0 ms spin lock) was obtained from the relation $I_0(\Omega_0) = I_{ref} k(\Omega_0)$ where $k(\Omega_0)$ is calculated for each spin from a simulation of the evolution of magnetization during the course of the adiabatic pulses (from the Z-axis to the effective field and back) by numerical solution of the Bloch equations, using experimental, residue specific ^{15}N R_1 and R_2 values, and neglecting the effects of chemical exchange. The 5 experimental values of I_0 and the $k(\Omega_0)$ profile for each residue were used to obtain I_{ref}. Figure 1 illustrates the $I_1(\Omega_0)$ profile for Gly 110 of L99A (open circles), along with the 5 experimentally determined $I_0(\Omega_0)$ values (open squares) and the simulated $I_0(\Omega_0)$ profile (dashed line), calculated as described above. Similar profiles have been obtained for all well resolved residues in L99A. Cross-peak intensities in $R_{1\rho}$ spectra were obtained by three-way decomposition of a 3D data set comprised of the series of 2D relaxation spectra as a function of Ω_0 using the MUNIN approach (Orekhov et al., 2001; Korzhnev et al., 2001), with the errors in $R_{1\rho}$ rates calculated from the signal to noise ratio in spectra.

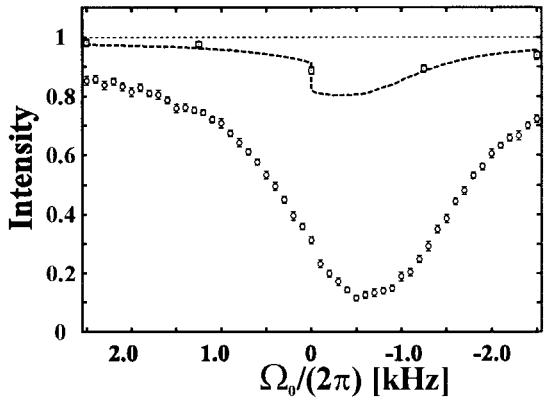

Figure 1. Intensity profile as a function of offset of the spin lock carrier from the center of the ^{15}N spectrum (119 ppm), $I_1(\Omega_0)$, measured for Gly 110 in L99A. A series of 51 spectra were recorded with a spin-lock field strength $\omega_1/(2\pi)$ of 805 Hz. Circles in the plot denote peak intensities I_1 in spectra recorded with a spin-lock duration of 60 ms (errors are indicated by the vertical bars), while squares indicate peak amplitudes I_0 at zero spin-lock length, i.e., after application of adiabatic pulses which rotate magnetization from the Z-axis to the effective field and back (5 points). The $I_0(\Omega_0)$ profile was generated from simulations of the evolution of magnetization during the adiabatic pulses using the Bloch equations, along with the 5 experimentally derived intensities. See text for details.

Results and discussion

In the present paper we analyze ^{15}N off-resonance spin-lock relaxation dispersion data recorded on the L99A mutant of T4 lysozyme. The substitution of Ala for Leu at position 99 creates a cavity of 150 Å^3 in the interior of the protein (Eriksson et al., 1992) which is able to bind relatively large ligands such as substituted benzenes (Morton and Matthews, 1995) with rates that vary from 325 s^{-1} (indole) to 800 s^{-1} (benzene), 20 °C (Feher et al., 1996). Previous relaxation dispersion studies based on the CPMG method have shown that L99A undergoes millisecond time-scale excursions to a partially disordered low-populated state, facilitating ligand entry into the cavity (Mulder et al., 2001a). Data recorded at both backbone amide ^{15}N and side chain methyl ^{13}C sites were found to be consistent with a single two-state exchange process, characterized by an exchange constant, k_{ex}, of 1450 s^{-1} and an excited state population, p_B, of 3.4% at 25 °C. In addition to measuring the kinetic and thermodynamic parameters that describe the exchange process, insight into the structural changes that accompany the transition was obtained from the values of $|\Delta\omega|$ extracted from fits of the dispersion data. As described above, the signs of many of the shift changes could be obtained through a comparison of peak positions in pairs of HSQC and HMQC correlation maps recorded at a single spectrometer field or from a set of HSQC spectra obtained at several different fields (Skrynnikov et al., 2002).

The large amount of information available on the L99A exchanging system makes it an attractive one to verify some of the features of $R_{1\rho}$ relaxation that are predicted by the Trott/Palmer theory, Equation 4. In particular, in comparing the equation of Davis et al. (Equation 5) which quantifies $R_{1\rho}$ in the limit of fast exchange with the more general result of Trott and Palmer it is clear that substantial differences are ex-

pected in the positions of extrema in $R_{1\rho}(\Omega_0)$ and $R_{ex}(\Omega_0)$ profiles. Many of the backbone ^{15}N spins in L99A that are in exchange are outside of the fast limit (Mulder et al., 2001a), and can be used to provide experimental verification of Equation 4. With this in mind we have measured detailed $R_{1\rho}(\Omega_0)$ profiles (51 points/curve) and demonstrate below that the experimental data are consistent only with the equation of Trott and Palmer.

Figure 2a shows the experimental $R_{1\rho}(\Omega_0)$ profile for the backbone ^{15}N of Gly 110 (open circles) measured using a spin lock field of 805 Hz. CPMG based methods and experiments which measure relative peak positions in HSQC/HMQC spectra have established that this residue has a large shift difference between exchanging states (5.3 ppm), with the shift of the minor conformer downfield that observed in the ground state. The solid and dashed lines in the plot correspond to the best fits of the $R_{1\rho}$ rates using the equations of Trott and Palmer (2002) and Davis et al. (1994), respectively, with k_{ex} and p_B fixed to the values obtained previously (1450 s^{-1}, 3.4%). It is noteworthy that we have not attempted to fit the data using all of the exchange parameters as free variables since, as described above, in the limit that $p_A \gg p_B, k_{ex}^2 \ll \omega_1^2$, valid in the present study, values of p_B and k_{ex} cannot be obtained separately. The profiles are, therefore, fit with $\Delta\omega$ and R_2 as adjustable parameters only. Values of $\Delta\tilde{\omega} = 4.6 \pm 0.5$ ppm, 6.0 ± 0.1 ppm are obtained using Equations 5 (Davis) and 6 (Trott and Palmer), respectively, in reasonable agreement with 5.3 ppm reported previously.

It is clear from Figure 2a that the best fit profile based on the equation of Davis et al. (Equation 5) is not in good agreement with the experimental $R_{1\rho}$ data. In this model the offset dependence of $R_{1\rho}$ is predicted to be symmetric about $\Omega = p_A\Omega_A + p_B\Omega_B$, typically taken as the observed peak position in HSQC spectra. ^{15}N $R_{1\rho}$ rates for Gly 110 predicted using this formula exhibit systematic deviations from the experimentally measured values. In particular, $R_{1\rho}$ rates are overestimated for spin-lock carrier values upfield of the ^{15}N resonance frequency of Gly 110 ('b' in Figure 2a) and underestimated for values of the carrier downfield of the position marked by 'a'. The maximum of the experimental $R_{1\rho}$ profile is shifted downfield with respect to the observed ^{15}N resonance frequency of Gly 110 (major state) towards the Larmor frequency of the unobservable minor state. The expressions of Trott and Palmer (Equations 3, 4) provide a good fit to the experimental $R_{1\rho}$ data and, importantly, predict

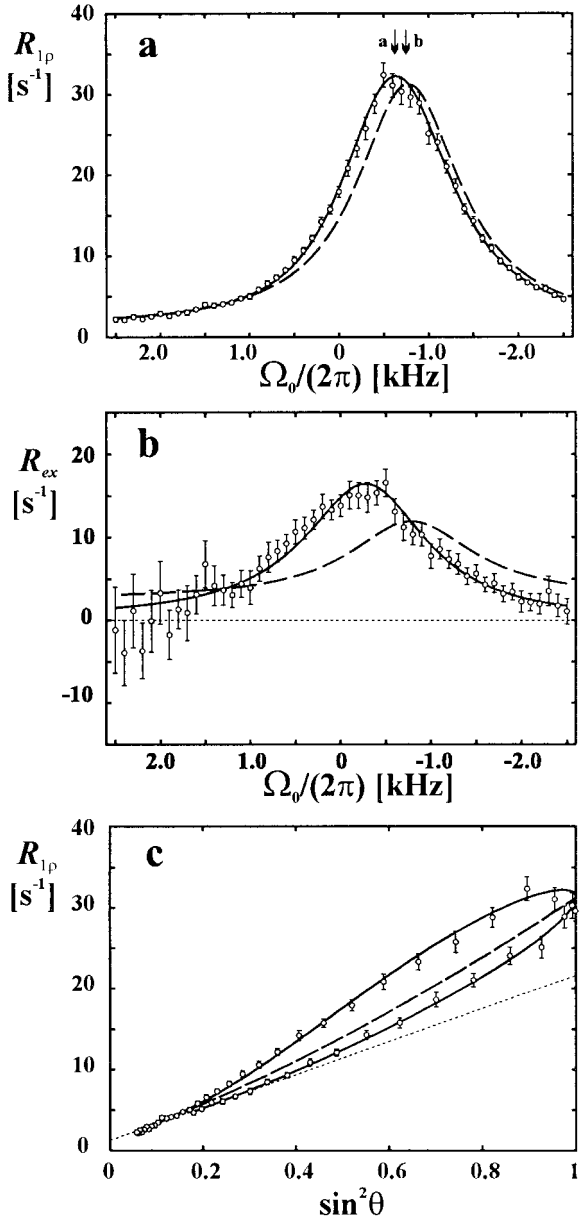

Figure 2. Experimentally derived off-resonance relaxation dispersion data for the backbone ^{15}N of Gly 110, L99A, measured with a spin-lock field strength, $\omega_1/(2\pi)$, of 805 Hz (open circles) along with fits of the data using the equations of Trott and Palmer (Equations 3, 4; solid lines) and Davis et al. (Equations 3, 5; dashed lines). Plots **a** and **b** show $R_{1\rho}$ and R_{ex} (calculated from $R_{1\rho}$ using Equation 3 with R_2 set to the value obtained from Equations 3, 4) values, respectively, as a function of the offset Ω_0 of the spin-lock carrier from the center of the ^{15}N spectrum, 119 ppm. Plot **c** shows $R_{1\rho}$ as function of sin$^2\theta$, where $\theta = \text{arccot}(\delta/\omega_1)$, $\delta = \Omega - \Omega_{SL}$, Ω_{SL} is the spin-lock carrier frequency and $\Omega = p_A\Omega_A + p_B\Omega_B$ is the population averaged Larmor frequency of the exchanging states. The dotted line indicates the expected $R_{1\rho}$ *vs.* sin$^2\theta$ profile in the absence of chemical exchange. All of the data was fit assuming values of 1450 s^{-1} and 3.4% for k_{ex} and p_B, respectively, obtained from CPMG dispersion measurements (Mulder et al., 2001a).

the correct shift of the $R_{1\rho}$ maximum ('a' in Figure 2a) with respect to the observed peak position of the major state ('b').

Figure 2b shows the exchange contribution, R_{ex}, to the transverse ^{15}N relaxation rate, R_2, of Gly 110 calculated from experimental ^{15}N $R_{1\rho}$ data using Equation 3 along with Equation 4 (solid line) or Equation 5 (fast exchange limit, dashed line). Values of k_{ex} and p_B obtained from CPMG relaxation studies, along with best fit $\Delta\tilde{\omega}$ values of 6.0 and 4.6 ppm generated from fits of $R_{1\rho}(\Omega_0)$ profiles (Figure 2a), were employed in the analysis. The R_{ex} profile for Gly 110 calculated using the Trott/Palmer formula is in good agreement with the experimental data, with a maximum shifted by $\Delta\omega/(2\pi) \sim 500$ Hz downfield with respect to the ^{15}N resonance position of the major conformer, located at the resonance frequency of the minor state (see Equation 6). In contrast, the profile generated using the equation valid in the fast-exchange limit which predicts a maximum at $\Omega = p_A\Omega_A + p_B\Omega_B$, does not fit the experimental data.

Exchange outside of the fast limit is easily identified by a plot of $R_{1\rho}$ as a function of $\sin^2\theta$ (Figure 2c). In the absence of exchange $R_{1\rho} = R_1\cos^2\theta + R_2\sin^2\theta$ is a linear function of $\sin^2\theta = \omega_1^2/\omega_e^2$, where $\omega_e^2 = \omega_1^2 + \delta^2$, $\delta = \Omega - \Omega_{SL}$, and is equal to R_1 at $\theta = 0$, 180° and to R_2 at $\theta = 90°$ (dotted line in Figure 2c). If exchange takes place a plot of $R_{1\rho}$ *vs.* $\sin^2\theta$ deviates from linearity due to the additional dependence of $R_{1\rho}$ on R_{ex} (note that R_{ex} also has a dependence on offset, Equations 4, 5 and Figure 2b). In the case of fast exchange R_{ex} depends only on $|\delta|$ and a single $R_{1\rho}$ value is obtained for each value of $\sin^2\theta$ (dashed line in Figure 2c). Outside of the fast exchange limit R_{ex} values clearly depend on the sign of δ (Equation 4) with larger R_{ex} rates observed in cases where the spin-lock carrier is closer to the resonance position of the minor conformer. Therefore, the $R_{1\rho}$ profile forms a loop with two different values of $R_{1\rho}$ obtained for each value of $\sin^2\theta$, as is easily observed for ^{15}N data from Gly 110 (solid line in Figure 2c).

Building on the results obtained for Gly 110 and our confidence in the Trott/Palmer equation to analyze $R_{1\rho}$ rates outside of the fast exchange regime, we have fit ^{15}N data from all residues in L99A that show exchange using Equation 4. In the fits $\Delta\omega$ and R_2 were treated as adjustable parameters, with k_{ex} and p_B fixed to 1450 s^{-1} and 3.4%, respectively (Mulder et al., 2001a), as described for Gly 110 above. Interestingly, optimization of the χ^2 target function (Press, 1997) for most of the residues showing conformational

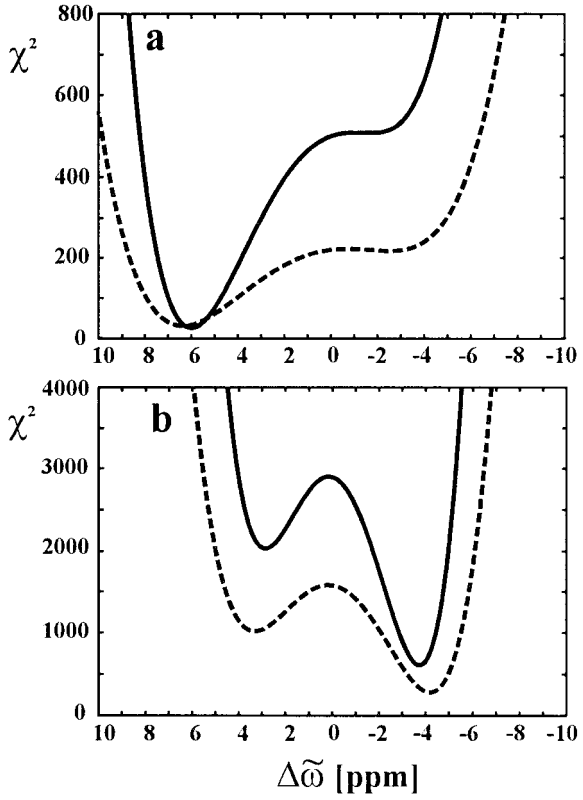

Figure 3. Dependence of the χ^2 target function on the chemical shift difference between the exchanging states $\Delta\tilde{\omega}$ in fits (Equations 3, 4) of ^{15}N $R_{1\rho}(\Omega_0)$ data for (a) Gly 110 and (b) Lys 135 in L99A. Solid and dashed lines show χ^2 profiles for the data measured with spin-lock field strengths, $\omega_1/(2\pi)$, of 805 and 1136 Hz, respectively. For each value of $\Delta\tilde{\omega}$ $R_{1\rho}(\Omega_0)$ profiles were fit with k_{ex} and p_B fixed to 1450 s^{-1} and 3.4%, respectively, with R_1 values measured in an independent experiment and with an adjustable parameter for R_2. The population averaged Larmor frequency of the exchanging states, $\Omega = p_A\Omega_A + p_B\Omega_B$, used in the data analysis was estimated from peak positions in HSQC spectra and Equation 8.

exchange established the existence of two minima, Figure 3. In general, one of the extrema was usually associated with a significantly lower χ^2 value than the other, allowing selection of the appropriate value of $\Delta\omega$ using F-test statistics (Lloyd, 1980). In the limit of fast exchange, however, information about the sign of $\Delta\omega$ is lost and χ^2 minima of equal depths are observed at frequency values of $\pm\Delta\omega$.

Figure 4 shows the correlation of chemical shift differences in ppm, $\Delta\tilde{\omega}$, for the backbone ^{15}N nuclei of L99A obtained from $R_{1\rho}$ and CPMG dispersion measurements (Mulder et al., 2001a). $R_{1\rho}$ data recorded at $\omega_1/(2\pi) = 805$ Hz and 1136 Hz spin-lock fields were fit simultaneously, with values of k_{ex} and p_B fixed to those obtained from CPMG dispersion

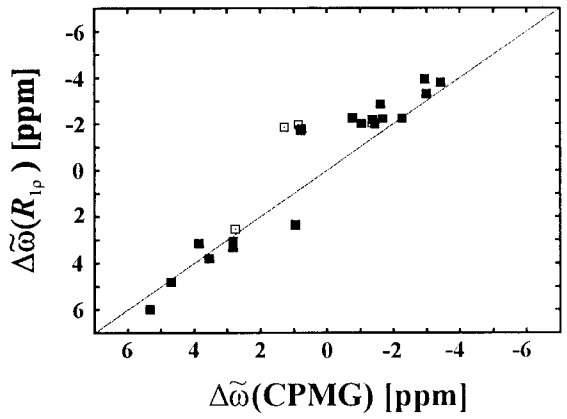

Figure 4. Comparison of chemical shift differences in ppm, $\Delta\tilde{\omega}$, between exchanging states for the backbone ^{15}N nuclei of L99A extracted from $R_{1\rho}$ data using the Trott/Palmer equation (Equations 3, 4) and from CPMG dispersion measurements (Mulder et al., 2001a). Values of $\Delta\tilde{\omega}$ obtained from $R_{1\rho}$ measurements were extracted by simultaneous fitting of data measured at two spin-lock field strengths, $\omega_1/(2\pi) = 805$ and 1136 Hz, using only the portion of the dispersion within ± 1.25 kHz of the maximum. (Very similar plots were obtained when the complete dispersions were fit.) In all fits of $R_{1\rho}$ data k_{ex} and p_B were set to 1450 s^{-1} and 3.4%, respectively. Each $R_{1\rho}$ fit was preformed with different starting values of $\Delta\tilde{\omega}$ and the solution corresponding to the deepest χ^2 minimum was always selected. Only data from those residues for which the Trott/Palmer equation (Equations 3, 4) improves the fit with respect to a model assuming no conformational exchange (at the 99.9% confidence level) is shown. Filled (open) squares show $\Delta\tilde{\omega}$ values for residues where one of the two χ^2 minima (see Figure 3) can (not) be selected with at least 99% confidence. In cases where a value of $\Delta\tilde{\omega}$ cannot be chosen with high confidence the value that gives the lowest χ^2 is plotted.

measurements, as described above. Note that analysis of the $R_{1\rho}$ data provides *both the magnitude and the sign* of the shift differences, $\Delta\tilde{\omega}$. The signs of $\Delta\tilde{\omega}$ (CPMG) values plotted in the figure are taken from a comparison of peak positions in HSQC/HMQC experiments (Skrynnikov et al., 2002).

In general a good correlation is observed between $\Delta\tilde{\omega}$ values extracted from $R_{1\rho}$ and CPMG data provided that $|\Delta\tilde{\omega}| \geqslant 2.5$ ppm (Figure 4). In many cases when values of $|\Delta\tilde{\omega}|$ less than 2.5 ppm were obtained from fits of the CPMG dispersion data, the corresponding fits of the $R_{1\rho}(\Omega_0)$ profiles using the Palmer/Trott formula did not show improvements relative to a model which assumes no exchange at the 99.9% confidence level (data not shown). For such nuclei the exchange contribution to $R_{1\rho}$ is largely suppressed even by the weak spin-lock fields used in our study. For example, the maximal exchange contribution to R_2 for an ^{15}N nucleus undergoing two-site exchange with $k_{ex} = 1450$ s^{-1} and $\Delta\tilde{\omega} = 2.5$ ppm is 2.8 s^{-1} for $\omega_1/(2\pi) = 805$ Hz and 1.5 s^{-1} for $\omega_1/(2\pi) = 1136$ Hz, on the order of the uncertainty of our $R_{1\rho}$ data. Finally, it is noteworthy that the correlations shown here are significantly improved over those obtained when $R_{1\rho}(\Omega_0)$ profiles measured with only a single ω_1 value are fit.

As described above, conformational exchange in the L99A system is better studied using CPMG-based experiments, since the exchange rate constant of this system, k_{ex}, falls in the range of ω_{CPMG} values that are typically used in ^{15}N CPMG dispersion measurements. In contrast, the k_{ex} value ($\sim$1500 s^{-1}) is considerably lower than ω_e values used in $R_{1\rho}$ experiments so that p_B and k_{ex} cannot be separated without additional information. The L99A system, does, however, allow us to evaluate the essential features of the Trott/Palmer equation and to establish its utility outside of the fast exchange regime.

In order to ascertain what the most favorable exchange regime might be for the extraction of k_{ex}, p_A (p_B) and $\Delta\omega$ exclusively from $R_{1\rho}$ data we have carried out a number of numerical simulations. Specifically, $R_{1\rho}$ data (800 MHz ^{1}H frequency) has been calculated for an ^{15}N nucleus with $\Delta\tilde{\omega} = 5.0$ ppm, $R_1 = 0.87$ s^{-1} and $R_2 = 15.8$ s^{-1} (corresponding to a backbone amide group attached to a protein tumbling isotropically with a correlation time of 10 ns). Pairs of $R_{1\rho}(\Omega_0)$ profiles were calculated, one for each of two spin-lock fields, $\omega_1/(2\pi) = 1$ and 1.5 kHz, as a function of k_{ex}, p_B. Each pair of profiles were fit simultaneously using the expression of Trott and Palmer (Equations 3, 4) in order to extract exchange parameters $(k_{ex})^{\mathrm{fit}}$, $(p_B)^{\mathrm{fit}}$ and $(\Delta\tilde{\omega})^{\mathrm{fit}}$, along with standard deviations of the extracted parameters, $\Delta(k_{ex})^{\mathrm{fit}}$, $\Delta(p_B)^{\mathrm{fit}}$ and $\Delta(\Delta\tilde{\omega})^{\mathrm{fit}}$, with respect to the input values estimated on the basis of the included errors in $R_{1\rho}$ rates, as described in the legend to Figure 5.

The results of the numerical simulations are presented in Figure 5, showing the ratios $\Delta(k_{ex})^{\mathrm{fit}}/k_{ex}$ (a), $\Delta(p_B)^{\mathrm{fit}}/p_B$ (b) and $\Delta(\Delta\tilde{\omega})^{\mathrm{fit}}/\Delta\tilde{\omega}$ (c), respectively, as a function of the input values of k_{ex} and p_B (recall that $\Delta\tilde{\omega}$ was set to 5 ppm in all simulations). Only those regions of k_{ex}, p_B space for which $\Delta(k_{ex})^{\mathrm{fit}}/k_{ex}$, $\Delta(p_B)^{\mathrm{fit}}/p_B$ and $\Delta(\Delta\tilde{\omega})^{\mathrm{fit}}/\Delta\tilde{\omega}$ do not exceed 1.0 are contoured in the figure. Figure 5d shows the maximum R_{ex} contribution to R_2 as a function of the input parameters k_{ex} and p_B, predicted by Equation 4. For large $\Delta\tilde{\omega}$ (5 ppm) k_{ex} on the order of 5000–10000 s^{-1} and $p_B > 3\%$, reasonably accurate rates and shift differences can be extracted

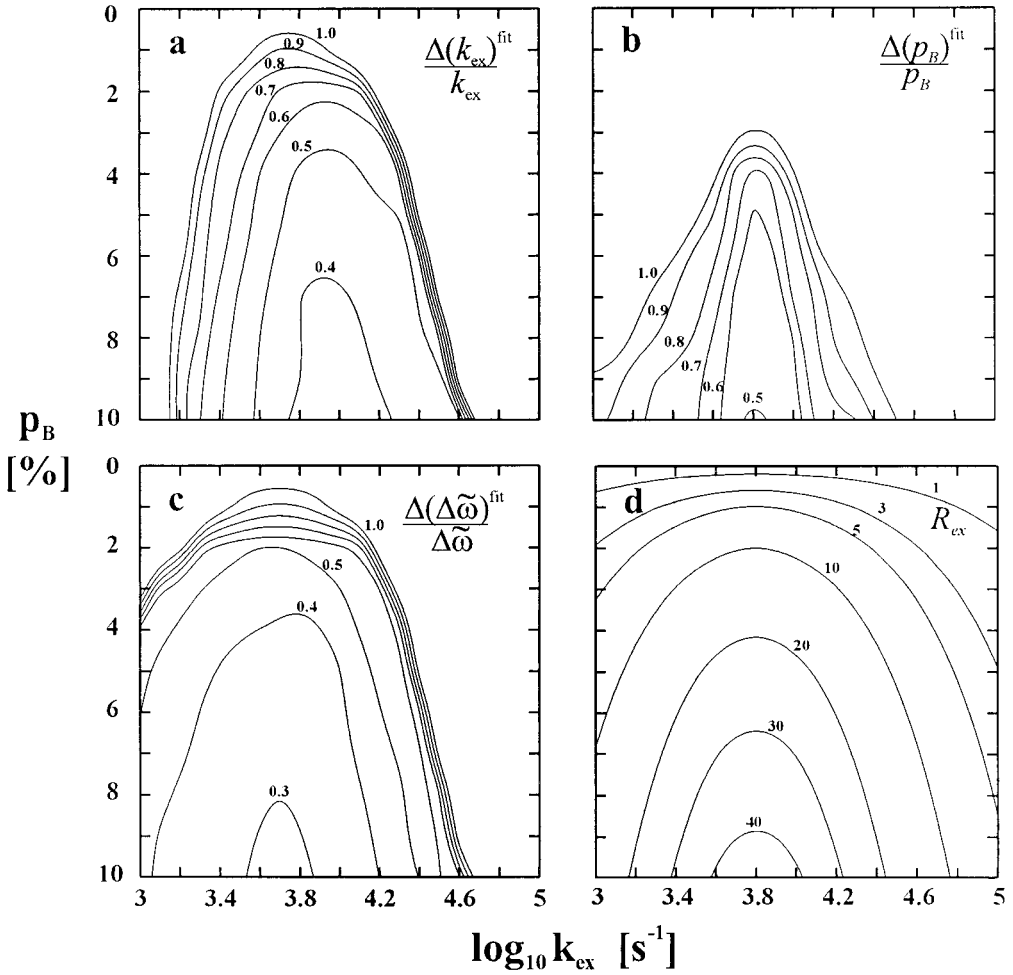

Figure 5. Contour plots of extracted exchange parameters from fits of simulated $R_{1\rho}(\Omega_0)$ rates. $R_{1\rho}$ values (800 MHz ^{1}H frequency) have been calculated from simulations of an ^{15}N nucleus ($R_1 = 0.87\ s^{-1}$ and $R_2 = 15.8\ s^{-1}$) undergoing two site exchange with $\Delta\tilde{\omega} = 5.0$ ppm. The decay profile of ^{15}N magnetization during the spin-lock period was comprised of 8 time points ranging from 0 to 120 ms and modeled by $M(t) = \exp(\lambda t) + g/s$, where λ is the least negative eigenvalue obtained by diagonalization of the evolution matrix **R** in Equations 1 and 2, g is a random number from a normal distribution with standard deviation of 1 (different random number for each time point) and s is the signal to noise ratio in spectra, assumed to be equal to 50. $R_{1\rho}$ values were extracted from fits of M(t) to a function of the form Aexp($-R_{1\rho}$t). $R_{1\rho}(\Omega_0)$ profiles consisting of 11 offsets ranging from -3 to 3 kHz ($\omega_1/(2\pi) = 1$ kHz) and -4 to 4 kHz ($\omega_1/(2\pi) = 1.5$ kHz) were calculated in this manner and subsequently fit using the expression of Trott and Palmer (Equations 3, 4) to extract the exchange parameters, $(k_{ex})^{fit}$, $(p_B)^{fit}$ and $(\Delta\tilde{\omega})^{fit}$. For each input value of k_{ex} and p_B the process was repeated a total of 200 times (with different random numbers 'g') so that root mean squared deviations of the extracted parameters, $\Delta(k_{ex})^{fit}$, $\Delta(p_B)^{fit}$ and $\Delta(\Delta\tilde{\omega})^{fit}$ with respect to the input values could be calculated. Only those model $R_{1\rho}$ data sets were used in the calculation of $\Delta(k_{ex})^{fit}$, $\Delta(p_B)^{fit}$ and $\Delta(\Delta\tilde{\omega})^{fit}$ where the Trott/Palmer model is selected over one which assumes no exchange (F-test confidence of 99%) in at least 25% of the cases. Plots **a**, **b** and **c** show the ratios $\Delta(k_{ex})^{fit}/k_{ex}$, $\Delta(p_B)^{fit}/p_B$ and $\Delta(\Delta\tilde{\omega})^{fit}/\Delta\tilde{\omega}$, respectively, as a function of input values of k_{ex} and p_B, while in **d** the dependence of the maximal exchange contribution to R_2 (in s^{-1}), as predicted by Equation 4, is illustrated.

($\Delta(k_{ex})^{fit}/k_{ex}$ and $\Delta(\Delta\tilde{\omega})^{fit}/\Delta\tilde{\omega}$ less than ~ 0.6), with somewhat larger errors in the extracted values of p_B. For k_{ex} values on the order of 1000 s^{-1}, k_{ex} and p_B values cannot be extracted with reasonable accuracy, as described above. Finally, for large values of k_{ex} ($\gtrsim \sim 20000\ s^{-1}$) the errors in the extracted parameters become large since the exchange contributions to R_2 are small.

In summary, we have presented an analysis of the offset dependence of backbone ^{15}N $R_{1\rho}$ rates for a mutant of T4 lysozyme which exhibits conformational exchange outside the fast limit. It is shown that

the expression for $R_{1\rho}$ derived recently by Trott and Palmer, valid over a wider range of time scales than previous descriptions which assumed fast exchange, is necessary to fit the majority of the experimental data. In cases where the exchange is outside the fast regime it is possible to obtain the sign of the shift difference between the exchanging sites. A reasonable correlation between shift differences obtained in the present study (based on $R_{1\rho}$ profiles) and those reported from a previous study using CPMG methods is obtained, especially considering the fact that the exchange kinetics of L99A are not ideally suited for analysis using rotating frame relaxation. Finally, numerical simulations have been performed which establish that at least in favorable exchange regimes and for large $\Delta\tilde{\omega}$ values it may be possible to extract all of the parameters describing a two-site exchange process from off-resonance spin-lock relaxation data recorded at a single spectrometer field.

Acknowledgements

The authors are grateful to Prof N.R. Skrynnikov (Purdue University) for useful discussions. V.Yu.O. acknowledges a STINT travel grant. The research was supported by a grant from the Canadian Institutes of Health Research. L.E.K. holds a Canada Research Chair in Biochemistry.

References

Akke, M. (2002) *Curr. Opin. Struct. Biol.*, **12**, 642–647.

Akke, M. and Palmer, A.G. (1996) *J. Am. Chem. Soc.*, **118**, 911–912.

Davis, D.G., Perlman, M.E. and London, R.E. (1994) *J. Magn. Reson. Ser. B*, **104**, 266–275.

Eriksson, A.E., Baase, W.A., Zhang, X.J., Heinz, D.W., Blaber, M., Baldwin, E.P. and Matthews, B.W. (1992) *Science*, **255**, 178–183.

Farrow, N.A., Muhandiram, R., Singer, A.U., Pascal, S.M., Kay, C.M., Gish, G., Shoelson, S.E., Pawson, T., Forman-Kay, J.D. and Kay, L.E. (1994) *Biochemistry*, **33**, 5984–6003.

Feher, V.A., Baldwin, E.P. and Dahlquist, F.W. (1996) *Nat. Struct. Biol.*, **3**, 516–521.

Guenneugues, M., Berthault, P. and Desvaux, H. (1999) *J. Magn. Reson.*, **136**, 118–126.

Korzhnev, D.M., Ibraghimov, I.V., Billeter, M. and Orekhov, V.Y. (2001) *J. Biomol. NMR*, **21**, 263–268.

Korzhnev, D.M., Karlsson, B.G., Orekhov, V.Y. and Billeter, M. (2003) *Protein Sci.*, **12**, 56–65.

Korzhnev, D.M., Skrynnikov, N.R., Millet, O., Torchia, D.A. and Kay, L.E. (2002) *J. Am. Chem. Soc.*, **124**, 10743–10753.

Lloyd, E. (1980) Statistics, Part A. In: *Handbook of Applicable Mathematics*, Ledermann, W., Ed. J. Wiley, Chichester, New York.

Loria, J.P., Rance, M. and Palmer, A.G. (1999a) *J. Am. Chem. Soc.*, **121**, 2331–2332.

Loria, J.P., Rance, M. and Palmer, A.G. (1999b) *J. Biomol. NMR*, **15**, 151–155.

McConnell, H.M. (1958) *J. Chem. Phys.*, **28**, 430–431.

Morton, A. and Matthews, B.W. (1995) *Biochemistry*, **34**, 8576–8588.

Mulder, F.A.A., de Graaf, R.A., Kaptein, R. and Boelens, R. (1998) *J. Magn. Reson.*, **131**, 351–357.

Mulder, F.A.A., Hon, B., Mittermaier, A., Dahlquist, F.W. and Kay, L.E. (2002) *J. Am. Chem. Soc.*, **124**, 1443–1451.

Mulder, F.A.A., Mittermaier, A., Hon, B., Dahlquist, F.W. and Kay, L.E. (2001a) *Nat. Struct. Biol.*, **8**, 932–935.

Mulder, F.A.A., Skrynnikov, N.R., Hon, B., Dahlquist, F.W. and Kay, L.E. (2001b) *J. Am. Chem. Soc.*, **123**, 967–975.

Orekhov, V.Y., Ibraghimov, I.V. and Billeter, M. (2001) *J. Biomol. NMR*, **20**, 49–60.

Orekhov, V.Y., Pervushin, K.V. and Arseniev, A.S. (1994) *Eur. J. Biochem.*, **219**, 887–896.

Palmer, A.G., Kroenke, C.D. and Loria, J.P. (2001) *Meth. Enzymol.*, **339**, 204–238.

Peng, J.W., Thanabal, V. and Wagner, G. (1991) *J. Magn. Reson.*, **94**, 82–100.

Press, W.H. (1997) *Numerical Recipes in C: The Art of Scientific Computing*, Cambridge University Press, Cambridge.

Skrynnikov, N.R., Dahlquist, F.W. and Kay, L.E. (2002) *J. Am. Chem. Soc.*, **124**, 12352–12360.

Skrynnikov, N.R., Mulder, F.A.A., Hon, B., Dahlquist, F.W. and Kay, L.E. (2001) *J. Am. Chem. Soc.*, **123**, 4556–4566.

Szyperski, T., Luginbuhl, P., Otting, G., Guntert, P. and Wüthrich, K. (1993) *J. Biomol. NMR*, **3**, 151–164.

Tollinger, M., Skrynnikov, N.R., Mulder, F.A.A., Forman-Kay, J.D. and Kay, L.E. (2001) *J. Am. Chem. Soc.*, **123**, 11341–11352.

Trott, O. and Palmer, A.G. (2002) *J. Magn. Reson.*, **154**, 157–160.

Trott, O., Abergel, D. and Palmer, A.G. (2003), *Mol. Phys.*, in press.

Zinn-Justin, S., Berthault, P., Guenneugues, M. and Desvaux, H. (1997) *J. Biomol. NMR*, **10**, 363–372.